CALCULATION OF EQUILIBRIUM PATHS IN NONLINEAR STRUCTURAL ANALYSIS

Sami Pajunen
Markku Tuomala

Rakenteiden Mekaniikka, Vol. 30.
Nro 1, 1997, s. 63-84

ABSTRACT

Methods for detecting and identifying limit and bifurcation points, continuing the equilibrium paths beyond limit points, handling bifurcation points and branch-switching are considered. Several methods have been programmed and numerical tests calculated in order to assess the various methods for handling both limit points and simple and multiple bifurcation points.

Key words: finite element method, equilibrium path, limit point, bifurcation.

INTRODUCTION

A general theory of structural stability was presented by Koiter for continuum problems already in 1945 [1]. Stability theory directly for discrete structural systems was developed in the sixties and seventies and those developments have been summarized in the book by Thompson and Hunt [2]. In nonlinear numerical structural analysis incremental iterative methods have been popular and successful. In the finite element method the solution of a structural problem can be presented as an equilibrium path in the (n+1)-dimensional space with n nodal point displacement degrees-of-freedom and a load parameter λ (assuming proportional loading). At limit points the path tangent is perpendicular to the λ-axis and Newton's iteration method parametrized by λ consequently breaks down. In addition the tangent stiffness matrix is singular at the limit point. At bifurcation points the tangent stiffness matrix is also singular and one or more secondary branches intersect the primary equilibrium path.

Methods for passing limit points have been presented widely in the mechanics literature [3-5]. Different path following methods have been studied e.g. in Ref. [6]. In the numerical mathematics literature the continuation methods have been studied since

the sixties and theoretical background for the methods has been developed [7-9].

At limit points the singularity of the stiffness matrix is not a serious problem. In practice, the probability to hit the limit point exactly is nil. Robust methods for handling limit points are presented e.g. in Refs. [11,29]. At bifurcation points the eigenvectors corresponding to the zero eigenvalue of the tangent stiffness matrix are solved and for branch-switching procedures based on utilizing the eigenvectors can be used [8,12,20,31]. Other methods, also capable of handling multiple bifurcation points have been presented [15-17]. At bifurcation points the singularity of the stiffness matrix is a more serious problem than in the case of limit points. In [11] the system of equations is regularized by a penalty method. Numerical analysts have developed special equation solving methods for handling the singularity at bifurcation points [12-14].

The different fundamental characteristics of structural stability can be studied by simple models, e.g. models consisting of bars and springs. Another useful class of analysis models comprise structural models for trusses, beams, frames and arches which have direct counterparts in building practice.

In the present work some of the above referenced studies are reviewed. A computer program has been made for continuing the solution path beyond limit points and also for handling bifurcation points and branch-switching. Both simple and multiple bifurcation points are considered. Several numerical test examples have been calculated in order to assess the different methods. Only elastic material behavior is considered in the present study.

EQUILIBRIUM EQUATIONS

In the total Lagrangian formulation the equation of virtual work for a deformable body is written with respect to its initial reference configuration in the form [18]

$$\int_V \mathbf{S}:\delta\mathbf{E}\,dV - \int_V \mathbf{b}\cdot\delta\mathbf{u}\,dV - \int_{S_t} \mathbf{t}\cdot\delta\mathbf{u}\,dS = 0\,, \tag{1}$$

where V is the volume of the body in its reference configuration, **S** is the second Piola-Kirchhoff stress tensor, **E** is the Green-Lagrangian strain tensor, **b** is the body force vector and the surface traction **t** is known on the part S_t of the boundary $S \equiv \partial V$. $\delta\mathbf{u}$ is the

virtual displacement vector with $\delta\mathbf{u}=\mathbf{0}$ on the part S_u of the boundary $S=S_u\cup S_t$.

The displacements of the body are interpolated by the shape functions $N_i(x)$ and the nodal point degrees-of-freedom $\mathbf{q}_i$ [19]:

$$\mathbf{u}(x) = \sum_i N_i \mathbf{q}_i \,. \tag{2}$$

Inserting (2) into the Green-Lagrangian strain formula [18] yields for virtual variables

$$\delta\mathbf{E} = \mathbf{B}\delta\mathbf{q}\,, \tag{3}$$

where $\mathbf{E}$ contains the strain components in vector form. By using Eqs. (2) and (3) the principle of virtual work gives the finite element equilibrium equations

$$\int_V \mathbf{B}^T\mathbf{S}dV - \int_V \mathbf{N}^T\mathbf{b}dV - \int_{S_t} \mathbf{N}^T\mathbf{t}dS = \mathbf{0}\,, \tag{4}$$

where $\mathbf{S}$ is a vector containing the components of the second Piola-Kirchhoff stress tensor, and it is indicated in (4) that $\mathbf{N}$ is a matrix containing the shape functions for the whole FEM-discretization. Equation (4) can be written in the form

$$\mathbf{g} \equiv \mathbf{r} - \mathbf{p} = \mathbf{0}\,, \tag{5}$$

in which

$$\mathbf{r} = \int_V \mathbf{B}^T\mathbf{S}dV \quad \text{and} \quad \mathbf{p} = \int_V \mathbf{N}^T\mathbf{b}dV + \int_{S_t} \mathbf{N}^T\mathbf{t}dS \tag{6}$$

are the internal force vector and the load vector, respectively. In practice, both $\mathbf{r}$ and $\mathbf{p}$ are assembled from the element contributions [19]. In the following it is assumed that all loads depend on a load factor λ in which case the equilibrium equations are

$$\mathbf{g}(\mathbf{q},\lambda) \equiv \mathbf{r}(\mathbf{q}) - \lambda\mathbf{p} = \mathbf{0}\,, \tag{7}$$

where $\mathbf{p}$ is a reference load vector. If there are n degrees of freedom in the finite element model, then $\mathbf{q}$ is a n-vector and $\mathbf{g}(\cdot,\cdot)$ is a nonlinear mapping from $\mathbf{R}^n\times\mathbf{R}\rightarrow\mathbf{R}^n$.

SOLUTION OF THE EQUILIBRIUM EQUATIONS

The nonlinear equilibrium equations (7) are usually solved incrementally by Newton's iteration method by using the load factor λ as a parameter:

$$\mathbf{K}_T(\mathbf{q}_k^i)d\mathbf{q}^{i+1} = \lambda_k\mathbf{p} - \mathbf{r}(\mathbf{q}_k^i)\,, \tag{8}$$

where $\mathbf{K}_T=\mathbf{g}_q$ is the tangent stiffness matrix, k and i denote the load step and iteration cycle numbers, respectively. In the updated Lagrangian formulation (UL) the reference configuration is updated to the equilibrium position of the body at the beginning of the increment. If the reference configuration is updated to the position attained at the latest iteration cycle then, in this study, the formulation is called Eulerian.

Continuation method in the presence of limit and bifurcation points

In figure 1 several solution branches are shown. Point A, where two branches intersect is a simple bifurcation point while point D is a multiple bifurcation point. Point B, at which $d\lambda/d\mathbf{q}=0$, is a limit point. Newton's iteration method parametrized by λ could skip over the bifurcation points but it would break down at the limit point B. Therefore, special procedures are needed for continuing the solution branch beyond limit points and for branch-switching at bifurcation points. The solution curve can be continued past limit points by augmenting the equilibrium equation (7) by a normalizing or constraint equation:

$$\begin{aligned} &\mathbf{g}(\mathbf{q},\lambda)=\mathbf{0}, \\ &c(\mathbf{q}(s),\lambda(s),s)=0, \end{aligned} \tag{9}$$

where the solution arc is parametrized by $s\in\mathbf{R}$. A smooth solution arc or branch of (9a) is a one-parameter family of solutions$(\mathbf{q}(s),\lambda(s))$ where $\mathbf{q}(s)\in\mathbf{R}^n$ and $\lambda(s)\in\mathbf{R}$. Several choices for the constraint equation have been proposed in the literature, e.g. [20]. For example the parameter s can be made to approximate the arclength of the solution curve and [8]:

$$c(\mathbf{q},\lambda,s)=\theta\mathbf{q}_0'\cdot(\mathbf{q}-\mathbf{q}_0)+(2-\theta)\lambda_0'(\lambda-\lambda_0)-(s-s_0)=0 \tag{10}$$

where θ is a weighting parameter $(0<\theta<2)$, $s\text{-}s_0$ is the step length with respect to s, differentiation with respect to s is denoted by a prime and $(\mathbf{q}_0,\lambda_0)=(\mathbf{q}(s_0),\lambda(s_0))$. The extended or constrained system of equilibrium equations (9) can be written in the form

$$\mathbf{G}(\mathbf{y},s)=\begin{Bmatrix}\mathbf{g}(\mathbf{q},\lambda)\\ c(\mathbf{q},\lambda,s)\end{Bmatrix}=\mathbf{0}, \tag{11}$$

where $\mathbf{y}=(\mathbf{q},\lambda)$. By the implicit function theorem the solution can be continued from a

known solution point $(\mathbf{q}_0,\lambda_0)$ if the Fréchet derivative or the Jacobian of **G** with respect to **y** is nonsingular.

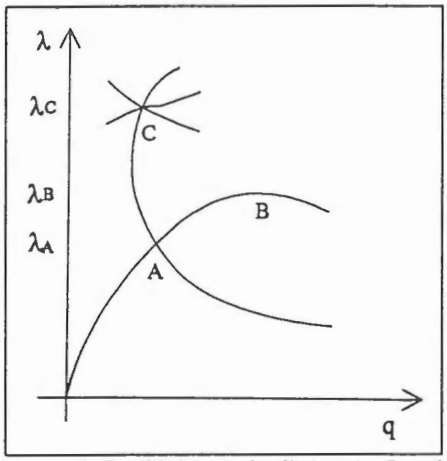

Figure 1. Equilibrium paths, limit point B and bifurcation points A and C

At regular points or limit points [17]

$$\mathbf{G}_y = \begin{bmatrix} \mathbf{g}_q(\mathbf{q},\lambda) & \mathbf{g}_\lambda(\mathbf{q},\lambda) \\ \mathbf{c}_q^T(\mathbf{q},\lambda,s) & c_\lambda(\mathbf{q},\lambda,s) \end{bmatrix} \tag{12}$$

is nonsingular if the vector $\mathbf{c}_q$ is not perpendicular to the tangent of the solution curve [17], i.e. the normal vector to the surface $c(\mathbf{y},s)=0$ must not be perpendicular to the tangent vector of $\mathbf{G}(\mathbf{y})=\mathbf{0}$. When Newton's method is applied to the extended system (11) it is obtained that

$$\begin{aligned} \mathbf{g}_q d\mathbf{q} + \mathbf{g}_\lambda d\lambda &= -\mathbf{g}, \\ \mathbf{c}_q^T d\mathbf{q} + c_\lambda d\lambda &= -c, \end{aligned} \tag{13}$$

where $\mathbf{g}_q=\mathbf{K}_T$ is the tangent stiffness matrix and $\mathbf{g}_\lambda=-\mathbf{p}$. In order to avoid the problems due to unsymmetry of the system (13) it can be solved in two parts [4,5,23]

$$\begin{aligned} d\mathbf{q}_p &= \mathbf{K}_T^{-1}\mathbf{p} \\ d\mathbf{q}_g &= \mathbf{K}_T^{-1}\mathbf{g} \end{aligned} \tag{14}$$

with

$$d\mathbf{q} = d\mathbf{q}_g + d\lambda d\mathbf{q}_p . \tag{15}$$

From (13b) and (15) $d\lambda$ can be solved:

$$d\lambda = -\frac{c + \mathbf{c}_q \cdot d\mathbf{q}_g}{c_\lambda + \mathbf{c}_q \cdot d\mathbf{q}_p} . \tag{16}$$

In the normal plane constraint method which is a special case of (10), Fig.2a,

$$\Delta\mathbf{q}^1 \cdot d\mathbf{q}^i + \Delta\lambda^1 d\lambda^i = 0, \tag{17}$$

an updated normal plane constraint is

$$\Delta\mathbf{q}^i \cdot d\mathbf{q}^{i+1} + \Delta\lambda^i d\lambda^{i+1} = 0, \tag{18}$$

where $\Delta\mathbf{q}^i = \mathbf{q}_{n+1}^i - \mathbf{q}_n$.

Corresponding to (18)

$$d\lambda^{i+1} = -\frac{\Delta q^i \cdot dq_g^{i+1}}{\Delta\lambda^i + \Delta q^i \cdot dq_p^{i+1}}. \tag{19}$$

Alternatively, Fried [30] has proposed a method in which (see Fig. 2b)

$$d\lambda^i = -\frac{dq_p \cdot dq_g^i}{1 + dq_p \cdot dq_p^i}. \tag{20}$$

An advantage of Fried's method is that the starting point of iteration does not have to be an equilibrium point [21].

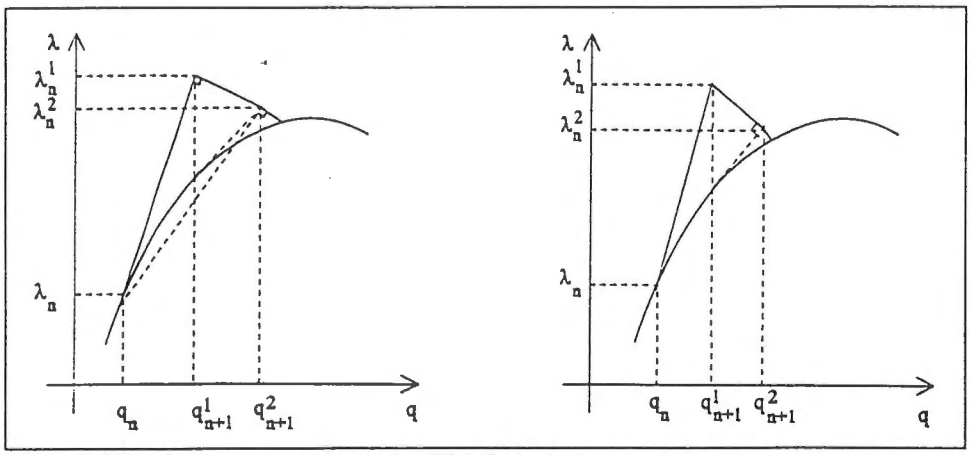

Figure 2. Normal plane constraint method and Fried's method.

Bifurcation points and branch-switching

At limit and bifurcation points the Jacobian

$$g_q^0 = g_q(q_0, \lambda_0) \tag{21}$$

is singular [8]. The null space of g_q^0 is spanned by linearly independent eigenvectors φ_i, i=1,...,m, where m is the multiplicity of the singular point. The null space is written as

$$\ker(g_q^0) = \text{span}\{\varphi_1, \ldots, \varphi_m\},\ \|\varphi_i\| = 1,\ i = 1, \ldots, m. \tag{22}$$

The range of g_q is defined by

$$\text{range}(g_q^0) = \{x \in R^n \,|\, \psi_i^T x = 0, i = 1, \ldots, m\}, \tag{23}$$

where the left eigenvectors ψ_i are chosen to satisfy

$$\psi_i^T \varphi_j = \delta_{ij}; \quad i,j = 1,\ldots,m. \tag{24}$$

The solution of (7) is studied near (q_0,λ_0) as a function of parameter s:

$$g(q(s),\lambda(s)) = 0 \tag{25}$$

with $(q(s_0),\lambda(s_0))=(q_0,\lambda_0)$. Differentiating (25) with respect to s yields

$$g_q^0 q_0' + g_\lambda^0 \lambda_0' = 0, \tag{26}$$

$$g_q^0 q_0'' + g_\lambda^0 \lambda_0'' = -(g_{qq}^0 q_0' q_0' + 2g_{q\lambda}^0 q_0' \lambda_0' + g_{\lambda\lambda}^0 (\lambda_0')^2) = 0, \tag{27}$$

where g_{qq}^0 is the second Fréchet derivative of g at (q_0,λ_0) and $q_0' = (dq/ds)|_{s=s_0}$. For the solution of (26) to exist it is required that $\lambda_0' g_\lambda^0 \in \text{range}(g_q^0)$, i.e. $\lambda_0' \psi_i^T g_\lambda^0 = 0$, which is possible if

$$g_\lambda^0 \in \text{range}(g_q^0) \quad \text{or} \quad g_\lambda^0 \notin \text{range}(g_q^0) \text{ but } \lambda_0' = 0. \tag{28}$$

In the first case (q_0,λ_0) is a bifurcation point and in the second case the critical point is a limit point. In the first case there is a unique solution v:

$$g_q^0 v + g_\lambda^0 = 0 \tag{29}$$

with

$$\psi_j^T v = 0, \quad j = 1,\ldots,m. \tag{30}$$

The general solution of (26) can be written in the form

$$q_0' = \xi_0 v + \sum_{j=1}^{m} \xi_j \varphi_j; \quad \xi_0 = \lambda_0'. \tag{31}$$

The existence of a solution for q_0'' in (27) requires that the right hand side belongs to the range of g_q^0, i.e.

$$\psi_i^T (g_{qq}^0 q_0' q_0' + 2g_{q\lambda}^0 q_0' \lambda_0' + g_{\lambda\lambda}^0 (\lambda_0')^2) = 0. \tag{32}$$

By inserting the solution (31) into (32) necessary conditions for the existence of a solution q_0'' are obtained [8]:

$$\sum_{k=1}^{m} \sum_{j=1}^{m} a_{ijk} \xi_j \xi_k + 2\sum_{j=1}^{m} b_{ij} \xi_j \xi_0 + c_i \xi_0^2 = 0, \; i = 1,\ldots,m, \tag{33}$$

where

$$a_{ijk} = a_{ikj} \equiv \psi_i^T g_{qq}^0 \varphi_j \varphi_k,$$
$$b_{ij} \equiv \psi_i^T (g_{qq}^0 v + g_{q\lambda}^0)\varphi_j, \tag{34}$$
$$c_j \equiv \psi_i^T (g_{qq}^0 vv + 2g_{q\lambda}^0 v + g_{\lambda\lambda}^0).$$

The homogenous polynomial equations are augmented with a normalization equation

$$\xi_0^2 + \xi_1^2 + \ldots + \xi_m^2 = 1. \tag{35}$$

In the case m=1 (33) reduces to

$$a\xi_1^2 + 2b\xi_1\xi_0 + c\xi_0^2 = 0, \tag{36}$$

where

$$a = \psi_1^T g_{qq}^0 \varphi_1 \varphi_1,$$
$$b = \psi_1^T (g_{qq}^0 v + g_{q\lambda}^0)\varphi_1, \tag{37}$$
$$c = \psi_1^T (g_{qq}^0 vv + 2g_{q\lambda}^0 v + g_{\lambda\lambda}^0).$$

Depending on the values of the coefficients, different type of behavior is obtained [22,11]. Define first $d=b^2-ac$. Accordingly, in the case of a bifurcation point:

$a \neq 0$, $d > 0$ gives transcritical bifurcation,
$a = 0$, $b \neq 0$ gives pitchfork bifurcation,
$d < 0$ gives isola formation.

For a limit point:

$a \neq 0$ corresponds a quadratic limit point,
$a = 0$ corresponds to a cubic limit point.

The coefficients a, b and c can be calculated analytically elementwise for some simple finite elements like for the truss element. In general case they can be obtained by numerical differentiation [8]. For positive d two sets of roots of the algebraic bifurcation equation (ABE) (36) can be solved and two tangents, one to the primary and one to the secondary path, can be constructed. A solution point $(\mathbf{q},\lambda)$ on any branch is stable if $\mathbf{g}_q$ is positive definite [26]. In the case of pitchfork bifurcation (a=0) the tangent vector of the primary path has the same direction as $\varphi_1 \equiv \varphi$, and the predictor step to the secondary path can be constructed as [23]

$$\delta_p \mathbf{q} = \xi \frac{\varphi}{\|\varphi\|}. \tag{38}$$

The scaling parameter ξ can be written in the form

$$\xi = \pm \frac{|q_{cr}|}{\tau}, \tag{39}$$

where the sign determines which branch of the secondary equilibrium path will be followed. If the displacements are small at the critical point, then τ is typically selected from the interval (0.5,5). In the case of large pre-buckling displacements a valid value for τ is typically between (5,100). If τ is chosen too small, the arc-length method converges back to the primary path and in the opposite case, with too large τ, the solution procedure diverges. When a point on the secondary path has been found, the path following can be continued. During the first steps there may be convergence difficulties because $\mathbf{K}_T$ is nearly singular. Reitinger and Ramm [24] have presented a modification of the previous procedure in which a perturbation is applied at the bifurcation point:

$$\bar{q} = q_0 + \xi \frac{\varphi}{\|\varphi\|} \quad . \tag{40}$$

A new tangent stiffness $\mathbf{K}_T(\bar{q})$ is formed at the perturbed state and path following is then started from the critical point.

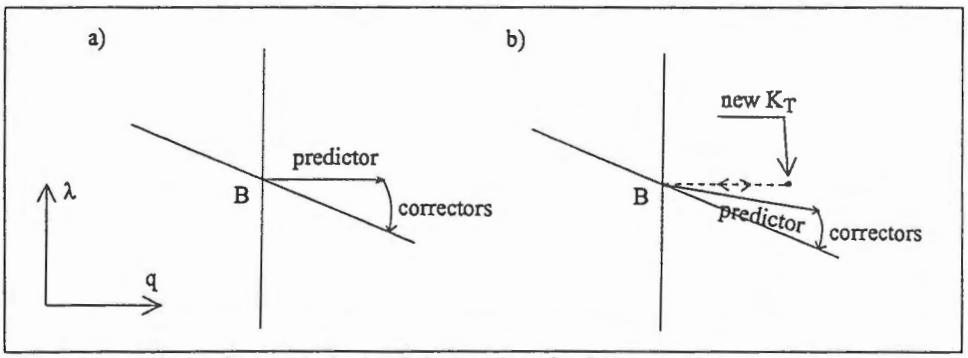

Figure 3. Branch-switching methods a) of Ref. 23, and b) of Ref. 24.

Especially in the case of multiple bifurcation points the use of ABE becomes increasingly difficult. In Refs. [16,17] a direct method for finding the arc directions at a bifurcation point $y_0=(q_0,\lambda_0)$ is given. If the arcs $y(s)$ passing through a m-fold bifurcation point are smooth functions of s, then their tangent vectors at $y=y(s_0)$ are in $\ker(G_y^0)=\text{span}\{\Phi_0, \Phi_1,...,\Phi_m\}$, where G_y^0 is the n+1 by n+1 Jacobi matrix of G and

$\Phi_i^T\Phi_j = \delta_{ij}$; i, j = 0,...,m , Φ_0 is an approximation for the tangent vector of the primary path. An affine space is given by

$$\Pi = \{y_0 + \sum_{j=0}^{m} \alpha_j \Phi_j | \alpha_j \in \mathbf{R}\}. \tag{41}$$

The direction vectors for arcs intersecting at y_0 are given by

$$t_i = \frac{m_i - y_0}{\|m_i - y_0\|}, \; i = 1,...,q, \tag{42}$$

where m_i, i=1,...,q, are the locations of the minima of $\|g\|$ on ∂A where $A \subset \Pi$ is a small region containing y_0. The region A can be chosen to be a (m+1)-ball of radius ε (B_{m+1}) centered at y_0. Figure 4 depicts the residual minimization technique in the two dimensional case.

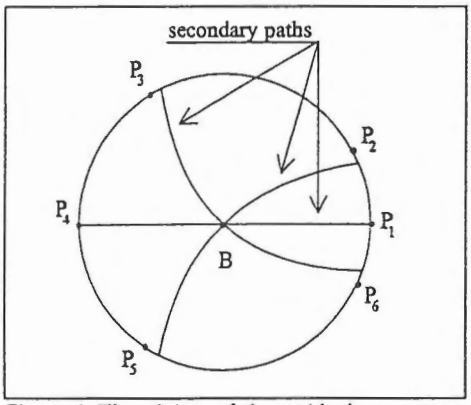

Figure 4. The minima of the residual vector g on ∂B_{m+1} and the projections of the secondary paths on the tangent plane at the bifurcation point.

Huitfeldt [17] has developed a method in which a perturbation problem is first formed:

$$g(y) + \tau d = 0, \tag{43}$$

where τ is a parameter and **d** is a vector. The problem (43) has a two-dimensional solution surface. The intersection of the surface and the sphere of radius ε around $(y_0,0)$ is a closed one-dimensional curve which passes one point on each branch of the unperturbed equation $g(y)=0$, and τ changes sign at the points of intersection. The curve can be followed by a continuation method for the problem

$$G(y,\tau) \equiv \begin{bmatrix} g(y) + \tau d \\ c(y,\tau) \end{bmatrix} = 0 \tag{44}$$

and points where τ=0 are searched. In the case of the spherical constraint

$$c(y,\tau) = \frac{1}{2}(\|y - y_0\|^2 + \tau^2 - \varepsilon^2). \tag{45}$$

Locating and identifying critical points

Consider simple critical points. The eigenvalues of the tangent stiffness matrix are calculated from

$$(\mathbf{K}_T - \omega \mathbf{I})\varphi = \mathbf{0}. \tag{46}$$

At a singular point one eigenvalue is zero and corresponding to that eigenvalue $\det\mathbf{K}_T=0$ and from (46) $\mathbf{K}_T\varphi=\mathbf{0}$. An extended system can now be formed for calculating the limit point at which $\varphi^T\mathbf{p}\neq 0$ [29,11]:

$$\mathbf{G}(q,\lambda,\varphi) = \left\{\mathbf{g}^T(q,\lambda) \quad (\mathbf{K}_T\varphi)^T \quad l(\varphi)\right\}^T = \mathbf{0}. \tag{47}$$

The last equation in (47) is a normalizing constraint, for example

$$l(\varphi) = |\varphi| - 1 = 0 \quad \text{or} \quad l(\varphi) = \mathbf{e}_i^T\varphi - \frac{\varphi_{0i}}{|\varphi_0|} = 0, \tag{48}$$

where $\mathbf{e}_i$ is the i:th basis vector in $\mathbf{R}^n$. The equation system (47) can be solved by a bordering algorithm without the necessity of actually solving the system of 2n+1 equations [13]. The solution of (47) converges quadratically towards the critical point and eigenvector. In this study a bisection method, e.g. [23] with the smallest pivot of $\mathbf{K}_T$ as a test function, has been used for detecting critical points on the equilibrium path. It is simpler than (47) but its convergence rate is linear.

At a critical point according to (28), (for simple critical points. Multiple limit point bifurcation is considered in [9]),

$$\lambda_0'\varphi^T\mathbf{g}_\lambda = 0 \quad \text{or} \quad \Delta\lambda_0\varphi^T\mathbf{p} = 0, \tag{49}$$

where $\Delta\lambda = \lambda'\Delta s$ and $\mathbf{p} = -\mathbf{g}_\lambda$. At a limit point $\lambda' = 0$ and at a bifurcation point

$$\varphi^T\mathbf{p} = 0. \tag{50}$$

The current stiffness parameter

$$S_p = \frac{\Delta\lambda_k\Delta\mathbf{q}_1\cdot\mathbf{p}}{\Delta\lambda_1\Delta\mathbf{q}_k\cdot\mathbf{p}} \tag{51}$$

introduced in [10] goes to zero when a limit point is approached. Therefore S_p can be used in detecting limit points. However, it cannot be used in finding bifurcation points. At a limit point the path tangent and the eigenvector φ have the same direction. Near the critical point the path tangent can be approximated by

$$\mathbf{t} = \frac{\mathbf{q}_{cr} - \mathbf{q}_{n-1}}{\left|\mathbf{q}_{cr} - \mathbf{q}_{n-1}\right|}, \tag{52}$$

where $\mathbf{q}_{n-1}$ is the last calculated point before the critical point. A test function for the critical point can also be defined by

$$\alpha = \arccos(\mathbf{t} \cdot \boldsymbol{\varphi}) \tag{53}$$

where $|\boldsymbol{\varphi}| = 1$ and α can obtain values between 0° and 180 °. If α is small, the critical point is identified as a limit point. However, the determination of the tangent vector $\mathbf{t}$ near the critical point may be sensitive to the chosen step length in some complex cases. Computation of the test functions is not costly. Therefore, for maximum reliability, one should use all available information when identifying the critical points.

SOME ONE-DIMENSIONAL FINITE ELEMENTS

Truss element

A total Lagrangian truss element is obtained by linear interpolation of the displacement components in a local (x,y,z)-coordinate system, where x is the bar axis and L is the element length:

$$u=N_1u_1+N_2u_2,\ v=N_1v_1+N_2v_2,\ w=N_1w_1+N_2w_2,\ \text{where } N_1=1-x/L,\ N_2=x/L. \tag{54}$$

The only component of the Green-Lagrangian strain tensor is

$$\varepsilon = u' + \frac{1}{2}u'^2 + \frac{1}{2}v'^2 + \frac{1}{2}w'^2, \tag{55}$$

where $\varepsilon \equiv E_{xx}$ in the local coordinate system and $(\,)' \equiv d(\,)/dx$. For an elastic bar $\sigma = E\varepsilon$. Inserting the displacement interpolation functions into the virtual strain formula yields

$$\delta\varepsilon = \mathbf{B}\delta\mathbf{q}, \tag{56}$$

where

$$\mathbf{B} = \left[(1+u')\mathbf{N}'\quad v'\mathbf{N}'\quad w'\mathbf{N}'\right] \text{ and } \delta\mathbf{q} = \left[\delta\mathbf{q}_u^T\quad \delta\mathbf{q}_v^T\quad \delta\mathbf{q}_w^T\right]^T, \tag{57}$$

i.e. $\delta\mathbf{q}$ is a 6×1 vector containing the virtual nodal point displacements and $\mathbf{N}=[N_1, N_2]$. The element contribution of the internal virtual work is

$$\int_{V_e} \sigma\delta\varepsilon dV = \delta\mathbf{q}^T \int_{V_e} \mathbf{B}^T \sigma dV, \tag{58}$$

where $\sigma \equiv S_{xx}$ is the only component of the second Piola-Kirchhoff stress tensor. The internal force vector of an element e is defined as

$$\mathbf{r}_e = \int_{V_e} \mathbf{B}^T \sigma dV . \tag{59}$$

Incrementing the right hand side of (59) yields the tangent stiffness matrix:

$$\int_{V_e} \mathbf{B}^T \Delta\sigma dV + \int_{V_e} \Delta\mathbf{B}^T \sigma dV = \mathbf{K}_T^e \Delta\mathbf{q} = (\mathbf{K}_{Tl}^e + \mathbf{K}_g^e)\Delta\mathbf{q} , \tag{60}$$

$$\mathbf{K}_{Tl}^e = \int_{V_e} \mathbf{B}^T \mathbf{E}\mathbf{B} dV \quad , \mathbf{K}_g^e = \int_{V_e} \mathrm{diag}\left[\mathbf{N}'^T \sigma \mathbf{N}' \quad \mathbf{N}'^T \sigma \mathbf{N}' \quad \mathbf{N}'^T \sigma \mathbf{N}'\right] dV . \tag{61}$$

In the algebraic bifurcation equation (36) the derivatives of g_q are needed. Denote [11]:

$$\mathbf{h} = (g_q \varphi)_q \Delta\mathbf{q} . \tag{62}$$

An analytical derivation for the derivatives of g_q is possible in the case of the truss element. Consider only the 2D-case in which

$$\sigma = E(u' + \frac{1}{2}u'^2 + \frac{1}{2}v'^2) \tag{63}$$

and

$$\mathbf{g}_q \varphi = \left\{ \int_{V_e} \mathbf{B}^T \mathbf{E}\mathbf{B} dV + \int_{V_e} \mathrm{diag}\left[\mathbf{N}'^T \sigma \mathbf{N}' \quad \mathbf{N}'^T \sigma \mathbf{N}'\right] dV \right\} \varphi . \tag{64}$$

$$\Rightarrow \mathbf{h}_e = (\mathbf{g}_q \varphi)_q \Delta\mathbf{q} = \int_{V_e} (\Delta\mathbf{B}^T \mathbf{E}\mathbf{B} + \mathbf{B}^T \mathbf{E}\Delta\mathbf{B} + \mathrm{diag}\left[\mathbf{N}'^T \Delta\sigma \mathbf{N}' \quad \mathbf{N}'^T \Delta\sigma \mathbf{N}'\right]) dV_e \varphi , \tag{65}$$

in which

$$\Delta\mathbf{B} = \left[\Delta u' \mathbf{N}' \quad \Delta v' \mathbf{N}'\right] \text{ and } \Delta\sigma = \mathbf{E}\Delta\varepsilon = \mathbf{E}\mathbf{B}\Delta\mathbf{q} . \tag{66}$$

From the above formulas it is now rather straightforward to compute the coefficients in the algebraic bifurcation equation in the case of 2D-truss.

Timoshenko beam elements

Consider a beam in a local (x,y)-coordinate system [27]. Assuming that the normals of the beam axis remain straight during deformation, the displacement components of an arbitrary point P of the cross section are

$$\begin{aligned} \mathfrak{u}(x,y) &= u(x) - y\sin\varphi(x), \\ \mathfrak{v}(x,y) &= v(x) - y(1-\cos\varphi(x)), \end{aligned} \tag{67}$$

where φ is the rotation of the cross section. The Green-Lagrangian strain components corresponding to (67) are

$$\begin{aligned} \varepsilon &= u' + \frac{1}{2}u'^2 + \frac{1}{2}v'^2 - y\varphi'[(1+u')\cos\varphi + v'\sin\varphi] + \frac{1}{2}y^2\varphi'^2, \\ \gamma &= -(1+u')\sin\varphi + v'\cos\varphi, \end{aligned} \tag{68}$$

where $\varepsilon \equiv E_{xx}$ and $\gamma \equiv 2E_{xy}$. Inserting the finite element interpolation formulas

$$u = \sum_i N_i u_i, \quad v = \sum_i N_i v_i, \quad \varphi = \sum_i N_i \varphi_i \tag{69}$$

into the virtual strain formulas yields

$$\begin{Bmatrix} \delta\varepsilon \\ \delta\gamma \end{Bmatrix} = \sum_{i=1}^{n_e} \mathbf{B}_i \delta\mathbf{q}_i, \quad \delta\mathbf{q}_i = \{\delta u_i \quad \delta v_i \quad \delta\varphi_i\}^T \tag{70}$$

contains the virtual displacements connected to node i.

The first part of the element tangent stiffness matrix is

$$\mathbf{K}_{T1}^e = \int_{V_e} \mathbf{B}^T \mathbf{D} \mathbf{B} dV, \quad \mathbf{D} = \mathrm{diag}[E \quad G], \tag{71}$$

when an elastic material is considered. The geometric stiffness matrix is obtained from

$$\int_{V_e} \Delta\mathbf{B}^T \mathbf{S} dV, \tag{72}$$

where $\mathbf{S}=[S_{xx}, S_{xy}]^T$ is the vector containing the Piola-Kirchhoff stress components. The strain-displacement matrices in (70a) containing trigonometric functions of rotation φ are highly nonlinear. By adapting an updated Lagrangian formulation the strain formulas can be simplified to incremental quantities

$$\begin{aligned} \Delta\varepsilon &= \Delta u' + \frac{1}{2}\Delta u'^2 + \frac{1}{2}\Delta v'^2 - y\Delta\varphi', \\ \Delta\gamma &= \Delta\varphi + \Delta v', \end{aligned} \tag{73}$$

where $\Delta\varepsilon$ and $\Delta\gamma$ are functions of the incremental displacements Δu and Δv between the configurations C_1 and C_2, where C_1 is an equilibrium configuration. The geometry is updated after every step when equilibrium is obtained. A very simple element capable of

modelling large displacement beam, frame and arch problems is obtained if linear interpolation is taken for u, v and φ.

NUMERICAL APPLICATIONS

Deep hinged arch

A hinged deep circular arch is depicted in Fig.5. The arch is modelled by 30 two-noded Timoshenko type frame/arch elements and the geometrical non-linearity is handled by the updated Lagrangian formulation. Fried's method is used for path following. It also works better than the normal plane method when the eigenmode injection technique is used for branch-switching. The calculated equilibrium paths are shown in Fig.5.

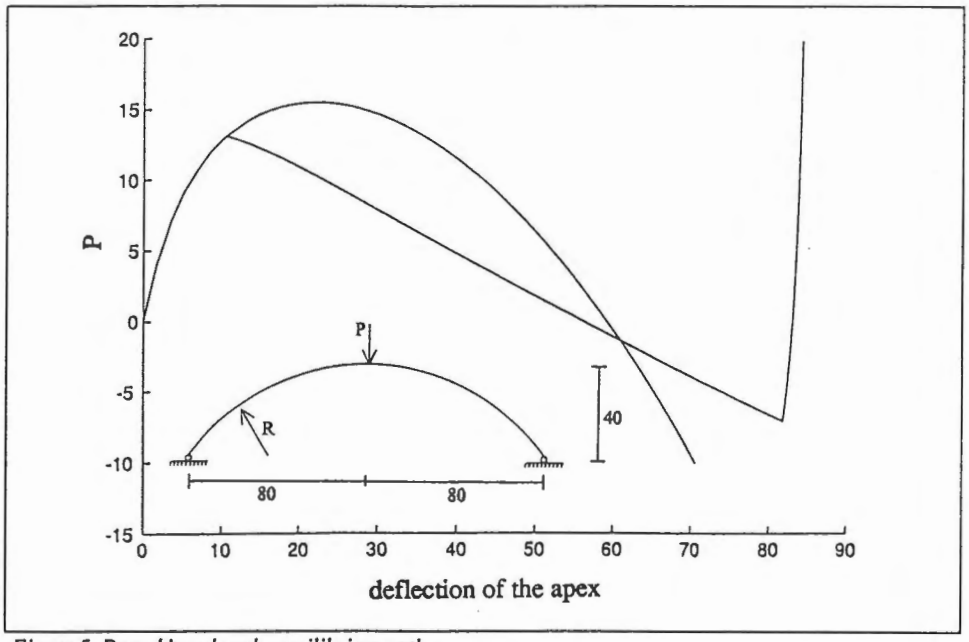

Figure 5. Deep hinged arch, equilibrium paths.

The techniques of references [23] and [24] performed well in branch-switching. The only difficulty observed, was in continuing after the limit point, if the first solution point was very near the limit point. Table 1. shows the values obtained at the different critical points of the example arch for the test functions (50), (51) and (53).

P_{cr}	S_p	$\frac{\varphi^T p}{\|\varphi\|\|p\|}$	*angle* α
13.1 (prim. path)	*0.14*	*1.20*	*33°*
15.5 (prim. path)	3.10^{-4}	*33.0*	*0.2°*
-7.1 (sec. path)	*2.00*	7.10^{-2}	*3°*

Table 1 . Test function values at critical points for the deep arch.

From Table 1 it can be seen that at the first critical point all the test functions have difficulties in identifying it as the bifurcation point, but if α=33° is not considered as a 'small' angle, then the test function α performs properly (the test function α needs further consideration: it must be tied to the step length and path curvature; for instance in axially compressed shells there can be rapid changes in the path curvature). The second critical point was identified as a limit point by all the test functions. However, at the third limit point S_p and the orthogonality test (50) did not act reliably. It should be noticed that all the three test functions are theoretically correct, but their behavior is sensitive for parameters (e.g. step length) of the used continuation method.

Symmetric two bar truss

The simple test structure, a two bar truss, depicted in Fig.6 is from [12]. The equilibrium paths are shown in Fig.6, too.

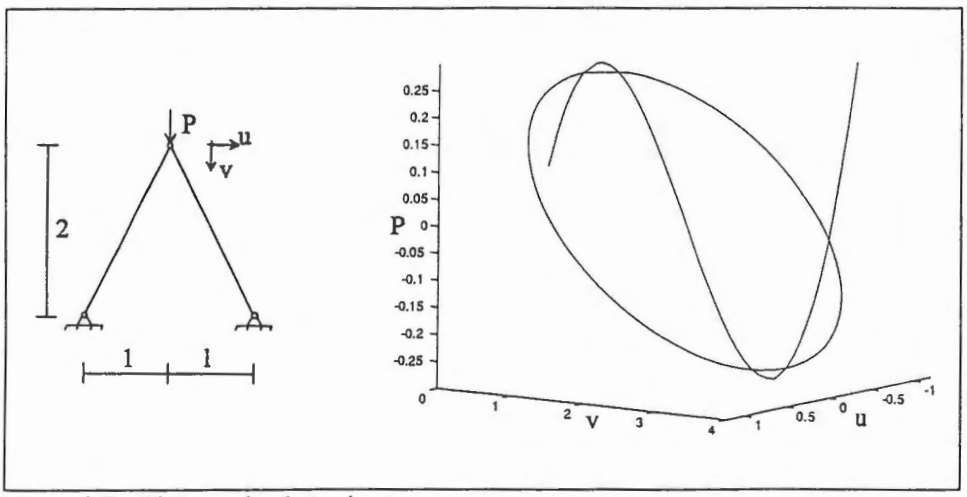

Figure 6. Equilibrium paths of a two bar truss.

At the first bifurcation point the vertical displacement is $v=2-\sqrt{2} \approx 0.5858$, which is obtained also by the numerical method. The bifurcations are of the symmetric pitchfork type and the coefficient a of the algebraic bifurcation equation is zero.

Asymmetric two bar truss

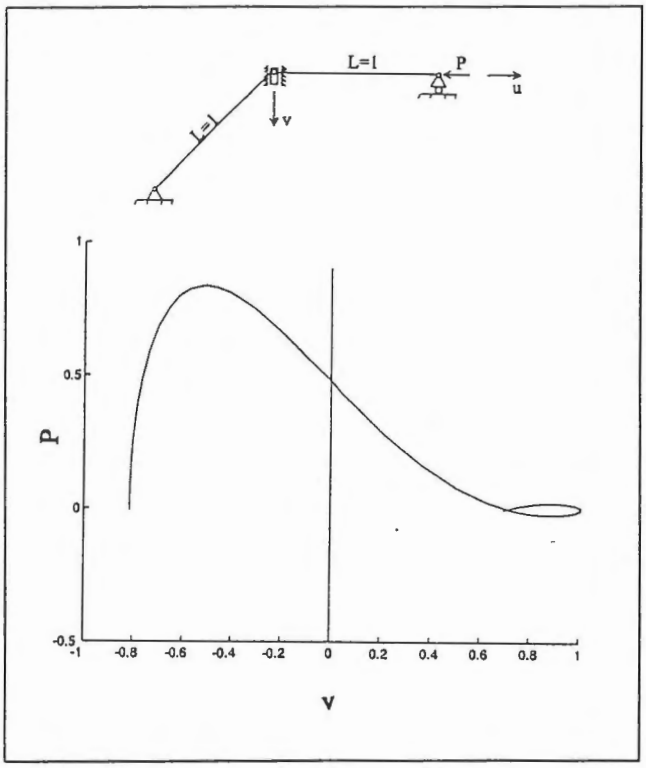

Figure 7. Asymmetric bifurcation problem.

Consider a plane structure consisting two bars, Fig.7. It is modified from a test example of Ref. [28]. The rigidity of the inclined bar is EA=1 and for the horizontal bar EA=10. With this example the branch-switching procedure based on ABE and the technique of Ref. [24] are tested. The structure exhibits trans-critical bifurcation as shown in Figure 7. In Table 2 the predictor-step values $\delta_p\lambda$, $\delta_p u$ and $\delta_p v$ for switching into the secondary path are given.

	ABE		Reitinger-Ramm	
	left branch	right branch	left branch	right branch
$\delta_p\lambda$	0.10	-0.10	0.10	-0.10
$\delta_p u$	$-6.30*10^{-4}$	$6.30*10^{-4}$	$-1.27*10^{-2}$	$1.14*10^{-2}$
$\delta_p v$	$-5.64*10^{-3}$	$5.64*10^{-3}$	$-8.57*10^{-2}$	$3.80*10^{-2}$

Table 2. Predictor-step values in branch-switching.

In the method of [24] the parameter value τ=5 was assumed and the step length in the arc-length method was 0.10. Both methods were successful in branch-switching. The method based on ABE gave a more accurate approximation to the secondary path.

Supported mast

A guyed mast structure shown in Fig.8 is used to test branch-switching at a double bifurcation point. Originally the mast example was constructed to model a double cusp catastrophe [25]. In the original study the mast was assumed infinitely rigid. In the present numerical test the structure was modelled by five 3D truss elements with rigidities EA=100 for the vertical bar and EA=$\sqrt{2}$ / 4 for the supporting inclined bars. The geometrical nonlinearity was taken into account by adopting the total Lagrangian formulation.

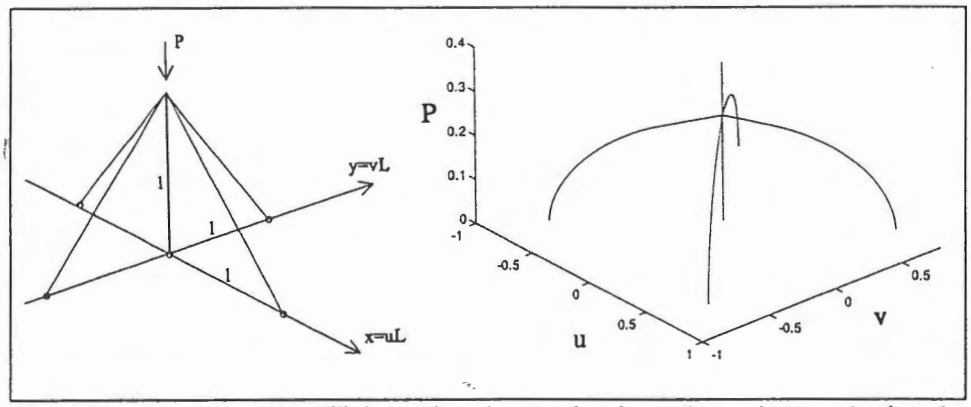

Figure 8. Supported mast and equilibrium paths: primary path and secondary paths emanating from the double bifurcation point.

In this example the residual minimization technique proposed by Kearfott [16] was used in locating the secondary paths by minimizing $\|g\|$, and it was combined with the technique of Ref. [23] in moving to the secondary path.

Shallow dome truss

A star-shaped dome truss is considered in this example. The dimensions are shown in Fig.9. The dome is loaded by several equal point forces placed symmetrically with

respect to the dome plan. The behavior of this seemingly simple example is, however, very complex. On the primary equilibrium path there are five bifurcation points and two limit points. Three of the bifurcation points are double critical points. By considering also the secondary branches, 51 bifurcation points can be found [26]. The finite element model consists of 24 3D truss elements with EA=1000. The equilibrium equations are formed by using the Eulerian description, and for path following Fried's method is still used. The primary path is followed beyond the first limit point and the secondary branches from the primary path are constructed. For the load parameter P the following critical values were obtained: 0.32, 0.50, 0.94 and 1.03, which are the same as reported by Healey [26]. The first critical point is a simple bifurcation point. After branch-switching a double bifurcation point was met on the secondary branch, at the load parameter value P=0.251. The second critical point P=0.50 on the primary path is a double bifurcation point, at which three secondary paths branch. Fig.10 shows a detail of the equilibrium paths in the vicinity of the critical point P=0.50.

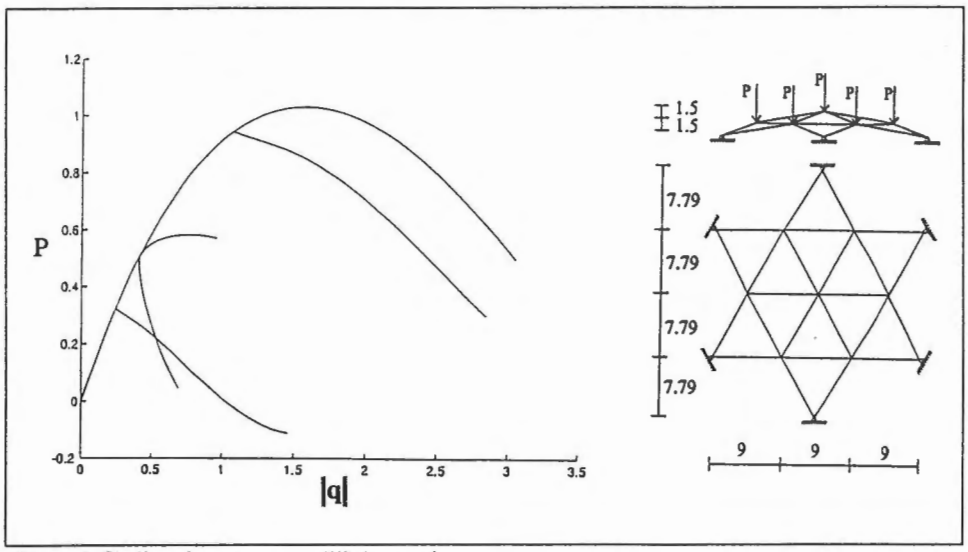

Figure 9. Shallow dome truss, equilibrium paths.

Healey [26] has obtained the equilibrium paths for the dome by constructing several reduced problems of the dome truss by group-theoretical considerations and by utilizing symmetry. Three different constrained structures can now be created so that the critical point P=0.50 becomes a simple bifurcation point for each substitute structure.

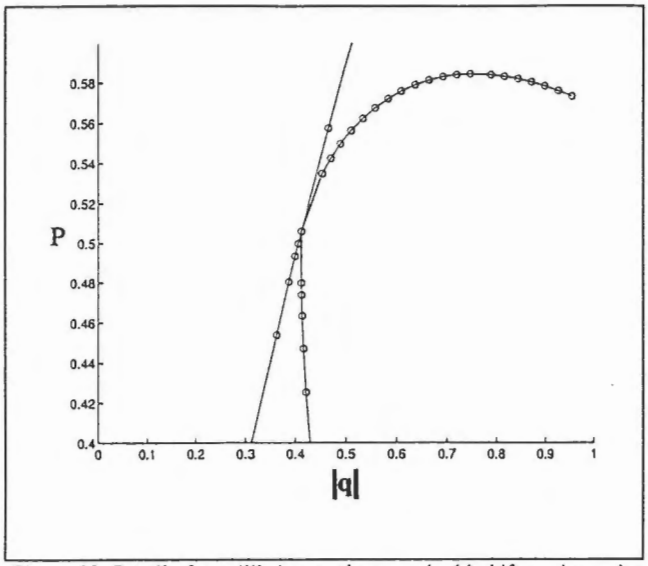

Figure 10. Detail of equilibrium paths near double bifurcation point at P=0.50.

The numerical methods had difficulties in switching to the lower secondary branch at P=0.50 but by applying constraints in the spirit of Healeys method it succeeded. Due to symmetry the three secondary paths look the same in the (P,|q|)-plane. Branch-switching at P=0.94 could be performed without difficulty.

CONCLUSIONS

The solution of non-linear equilibrium equations, the determination of equilibrium paths, the detection of limit and bifurcation points and branch-switching are considered. Several methods and techniques have been programmed into a computer program and test calculations have been performed on representative truss and arch example structures. For simple bifurcation points, especially for the most common type of symmetrical bifurcation, reliable branch-switching techniques exist. Tentatively, also some recently introduced techniques, capable of handling also multiple bifurcation points, have been considered. In the next stage more emphasis will be directed towards dealing with multiple bifurcation, and also the imperfection sensitivity will be studied by introducing an extra parameter into the equilibrium equations.

REFERENCES

1. KOITER W.T. 1945, *Over de Stabiliteit van het Elastisch Evenwicht*, PhD Thesis, Technisce Hogeschool, Delft. English translation: *AFFDL TR-7025* (1970).

2. THOMPSON J.M.T. & HUNT G.W. 1973, *A General Theory of Elastic Stability*, Wiley, London.

3. WEMPNER G.A. 1971, Discrete approximations related to the nonlinear theories of solids, *Int. J. Solids Struct.*, **7**, 1581-1599.

4. RIKS E. 1972, The application of Newtons method to the problem of elastic stability, *J. Appl. Mech.*, **39**, 1060-1066.

5. RAMM E. 1980, Strategies for tracing the nonlinear response near limit points, *Nonlinear Finite Element Analysis in Structural Mechanics*, Bathe K.J. & al. (eds.), Springer-Verlag, 63-89.

6. KOUHIA R. & MIKKOLA M. 1995, Strategies for structural stability analysis, *Advances in Finite Element Technology*, Wiberg N.E. (ed.), CIMNE, 254-278.

7. HASELGROVE C.B. 1961, The solution of non-linear equations and of differential equations with two point boundary conditions, *Computer J.*, **4**, 255-259.

8. KELLER H.B. 1977, Numerical solution of bifurcation and nonlinear eigenvalue problems, *Applications of Bifurcation Theory*, Rabinowitz P. (ed.), Academic Press, New York, 359-384.

9. DECKER D.W. & KELLER H.B. 1980, Multiple Limit Point Bifurcation, *J. Math. Anal. and Appl.*, **75**, 417-430.

10. BERGAN P.G. & HORRIGMOE G. & KRÅKELAND B. & SØREIDE T.H. 1978, Solution techniques for non-linear finite element problems, *Int. J. Num. Meth. Eng.*, **12**, 1677-1696.

11. WRIGGERS P. & SIMO J.C. 1990, A general procedure for the direct computation of turning and bifurcation points, *Int. J. Num. Meth. Eng.*, **30**, 155-176.

12. RHEINBOLDT W.C. 1977, Numerical continuation methods for finite element applications, *Formulations and Computational Algorithms in FE Analysis, Proc. U.S.-Germany Symposium*, Bathe K. J. & al. (eds.), 599-631.

13. KELLER H.B. 1983, The bordering algorithm and path following near singular points of higher nullity, *SIAM J. Sci. Stat. Comp.*, **4**, 573-582.

14. CHAN T.F. & RESASCO D.C. 1986, Generalized deflated block-elimination, *SIAM J. Numer. Anal.*, **23**, 913-923.

15. ALLGOWER E.L. & CHIEN C.-S. 1986, Continuation and local perturbation for multiple bifurcations, *SIAM J. Sci. Stat. Comput.*, **7**, 1265-1281.

16. KEARFOTT R.B. 1983, Some general bifurcation techniques, *SIAM J. Sci. Stat. Comput.*, **4**, 52-68.

17. HUITFELDT J. 1991, Nonlinear eigenvalue problems - prediction of bifurcation points and branch-switching, *Numerical analysis report 17*, Department of Computer Sciences, Chalmers University of Technology, Göteborg.

18. MALVERN L.E. 1969, *Introduction to the Mechanics of a Continuous Medium*, Prentice-Hall.

19. ZIENKIEWICZ O.C. & TAYLOR R.L. 1991, *The Finite Element Method, Vol 1 & 2*, McGraw-Hill, London.

20. KOUHIA R. & MIKKOLA M. 1989, Tracing the equilibrium path beyond simple critical points, *Int. J. Num. Meth. Eng.*, **28**, 2923-2941.

21. KOUHIA R. 1992, On the solution of non-linear finite element equations, *Computers & Structures*, **44**, 243-254.

22. SPENCE A. & JEPSON A.D. 1985, Folds in the solution of two parameter systems and their calculation, Part I, *SIAM J. Numer. Anal.*, **22**, 347-368.

23. WAGNER W. & WRIGGERS P. 1988, A simple method for the calculation of postcritical branches, *Eng. Comput.*, 5, 103-109.

24. REITINGER R. & RAMM E. 1995, Buckling and imperfection sensitivity in the optimization of shell structures, *Thin-Walled Structures*, **23**, 159-177.

25. GÁSPÁR ZS. 1977, Buckling models for higher catastrophes, *ASCE J. Struct. Mech*, **5**, No. 4.

26. HEALEY T.J. 1988, A group-theoretic approach to computational bifurcation problems with symmetry, *Comp. Meth. App. Mech. Eng.*, **67**, 257-295.

27. MIKKOLA M. & TUOMALA M. 1989, Mechanics of impact energy absorption, Helsinki University of Technology, Dept. of Struct. Eng., *Report 104*.

28. SHI J. 1996, Computing critical points and secondary paths in nonlinear structural stability analysis by the finite element method, *Computers & Structures*, **58**, 302-220.

29. WERNER B. & SPENCE A. 1984, The computation of symmetry breaking bifurcation points, *SIAM J. Numer. Anal.*, **21**, 388-399.

30. FRIED I. 1984, Orthogonal trajectory accession to the non-linear equilibrium curve, *Comp. Meth. Appl. Mech. Eng.*, **47**, 283-298.

31. ERIKSSON A. 1991, Derivatives of tangential stiffness matrices for equilibrium path descriptions, *Int. J. Num. Meth. Eng.*, **32**, 1093-1113.

Sami Pajunen
M.Sc., Researcher
Department of Civil Engineering
Tampere University of Technology
email: sami@junior.ce.tut.fi

Markku Tuomala
Professor
Department of Civil Engineering
Tampere University of Technology
email: markku@junior.ce.tut.fi